

MODELING RETENTION MECHANISMS IN TORE SUPRA CIEL LONG DISCHARGES

J Hogan¹, E Tsitrone², T. Loarer², P Thomas², R Mitteau² and the Tore Supra Team²

¹Oak Ridge National Laboratory, Fusion Energy Division, TN37831-8072, USA

²Association Euratom-CEA sur la fusion, C.E. Cadarache, 13108 St-Paul-lez-Durance, France

1. Introduction

High levels of deuterium retention have been observed in Tore Supra long discharges and models which might explain this are evaluated. Retention due solely to the implanted flux from locally charge-exchanged D in the footprint area near gas inlets is compared with retention due to co-deposition, using a core/SOL/wall integrated, coupled code system combining CASTEM-2000, BBQ and MIST/ITC.

2. Deuterium implantation model

In a representative Tore Supra long (260 s) discharge, an average D flux $\sim 5 \cdot 10^{20}$ particles/s is steadily injected into the system, and an average flux $2 - 2.5 \cdot 10^{20}$ particles/s is retained in the vessel, after accounting for core and actively pumped particles [1]. Due to charge exchange (CX) with plasma ions in the gas injection areas, a significant local flux of energetic D neutrals will be emitted and implanted in the local CX 'footprint'. Figure 1 (top) shows the calculated localization of the back-scattered and implanted flux, obtained using deuterium BBQ [2] for a port in the Tore Supra low-field side mid-plane. For calculations summarized here we assume electron density at the last closed magnetic surface $n_e(\text{LCMS}) = 4-7 \cdot 10^{18} \text{ m}^{-3}$, $T_e(\text{LCMS}) = 50-90 \text{ eV}$, and the scrape-off layer decay lengths for density (λ_N) and temperature (λ_T) are 5-50 mm and 10-50 mm, respectively. We further assume $T_i = T_e$. As seen in Fig. 1 (bottom), back-scattered D flux is highly localized within 0.1m of the inlet, with typical mean deposition energy (E_{dep}) of 40-100eV. The value of E_{dep} is sensitive to the unmeasured background T_i . The calculated D implantation flux would be large enough to account for the wall retention, if it were all retained. However, implanted D recycles after local saturation is reached, and the retained amount is proportional to the product of the CX

footprint area, implantation depth (increasing with E_{dep}) and the relative storage capacity of the aC:D layer (which depends on the type of surface - hard or soft). A global recycling coefficient (R) in the range of 0.1-0.2 at the end of the long discharge would be required to retain the implanted flux.

Models have thus been evaluated for hard (40% D:C retention, TRIM implantation range values), and soft films (up to 100% D:C retention, $\sim 1.5x$ TRIM range values) for several proposed wall saturation models: JET PTE-1, Ehrenberg, Moeller-Scherzer and Grisolia-Pegourie [see references in 3]. Figure 2 compares the approach to saturation, using both hard (2a) and soft (2b) film assumptions. For the most optimistic case (soft films, Grisolia-Pegourie et al model) saturation times in excess of 4 minutes are possible, yielding the low value of R which is needed for long pulse retention. However, other models predict much shorter saturation times, so we proceed to examine mechanisms for continuous C generation and D co-deposition.

3. Co-deposition and steady, non-equilibrium SOL carbon population

Under steady conditions C produced at the plasma-facing components enters a closed system and interacts several times with these surfaces before final deposition. A coupled core/SOL/wall code has been developed to analyze carbon pathways in this system [5]. Impurity generation from ion sputtering is calculated using an early version of CASTEM-2000, to provide starting C fluxes for the BBQ SOL code. New chemical and self-sputtering rates have been included. Figure 3a-d shows representative C emission fluxes for the new sputtering models calculated for a segment of the Tore Supra CIEL configuration. The BBQ-calculated influx to the core plasma provides boundary conditions for core radial transport codes MIST and ITC (MIST is used for the cases shown here). The calculated emergent flux from the core is then used, along with CASTEM self-sputtering rate profiles, in an iterative core-SOL calculation to find the predicted steady impurity content in the system.

The presence of non-thermal electrons in the SOL, from Lower Hybrid heating, increases the charge of SOL impurities (thus their sheath enhanced impact energy for self-sputtering) and consequently further increase the self-sputtering rate. Also, bond passivation,

due to the D flux co-deposited with C, can greatly increase the sputtering yield for heavy particles [4]. We can expect such an effect near a gas inlet, where there is a large flux of local CX particles. Figure 4a-f shows the evolution of the resulting C core density in the coupled system for 3 *ad hoc* fast electron localization models: just inside the last closed flux surface, in the mid- SOL, and in the far-SOL. A non-thermal electron population with 10% of the background thermal density, and an effective temperature of 200 eV is assumed. For each localization case, curves are shown assuming no self-sputtering, self-sputtering using TRIM self-sputtering values, and assuming an additional 3-fold increase in self-sputtering due to the local neutral flux. Figure 5 shows the radial profile of the non-equilibrium CVI SOL population from the case with TRIM self-sputter values and mid-SOL heating localization. The self-sputtering yield can be increased 10-fold (Fig. 3) for this population.

4. Conclusions

According to some wall retention models, retention of the CX-deposited neutral D flux near the gas injection port can account for the levels seen in long discharges. A large retention can also be due to D co-deposition with sputtered C. Sputtering from plasma-facing components can be enhanced by large self-sputtering rates due to non-equilibrium charge state distribution in the SOL, caused by localized heating, and further enhancement of the sputtering rate can be created by the co-existing neutral D flux. This model is obviously speculative at this stage, and detailed experimental investigation, focussing on the SOL, is needed for validation.

Acknowledgement: ORNL. Supported by U.S.DOE Contract DE-AC05-00OR22725.

References

- [1] E Tsitrone, D Reiter et al PSI 16 (to be published), E Tsitrone et al, EPS2003
- [2] A Escarguel, B Pegourie, J Hogan et al, PPCF **43** (2001) 1733
- [3] C Grisolia, J Hogan, J Nucl Mater **290-293** (2001) 402
- [4] J Hogan, E Tsitrone, et al EPS 2003
- [5] C Hopf, A. von Keudell, W. Jacob, Nuclear Fusion **42** (2002) L27-30

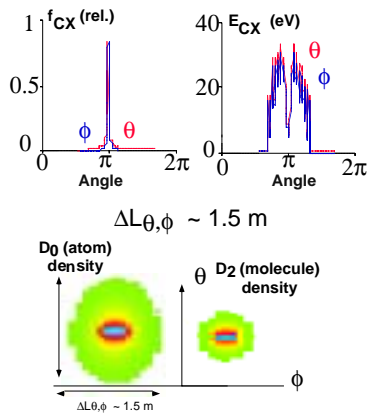


Figure 1. BBQ D results for CX implantation. Angular distributions of implanted flux, energy (top) and degree of localization for D₀, D₂ (bottom)

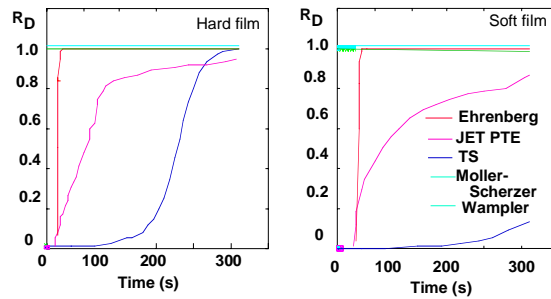


Figure 2. Comparison of saturation times for hard (left) and soft (right) film assumptions, for several models. Grisolia-Pegourie (blue) and JET PTE-1 (magenta) models show longest saturation times

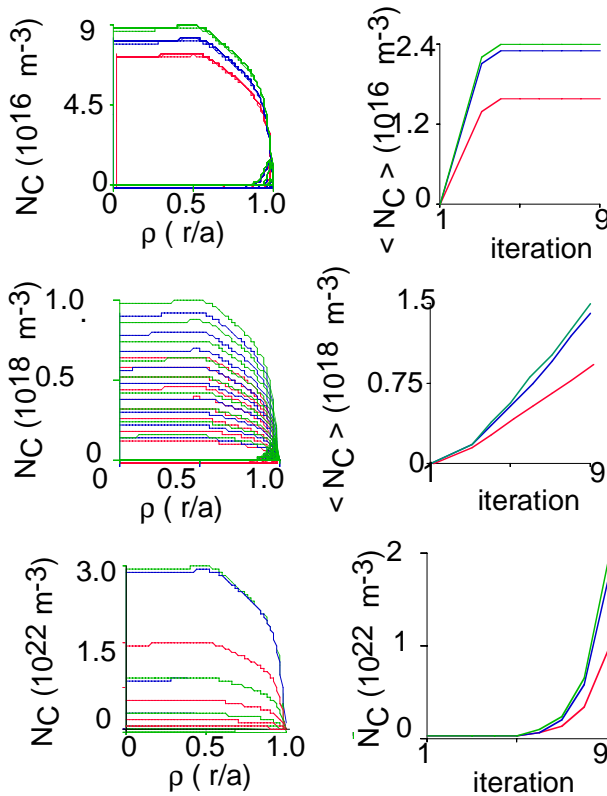


Figure 4. Core carbon density, volume average and profile evolution, for cases with no self-sputter (top), TRIM values (middle) and enhanced yield due to bond passivation. Each for cases with inner (red), mid- (blue) and far-SOL (green) localized heating.

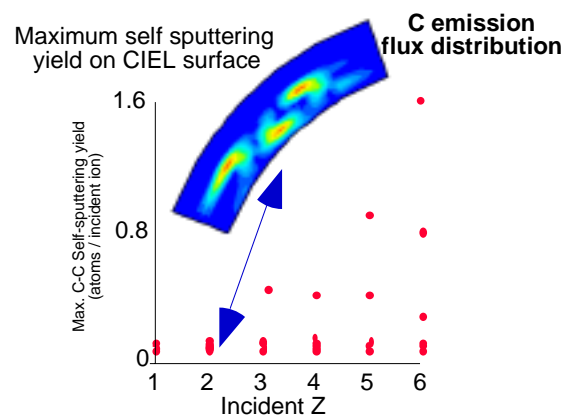


Figure 3. Maximum self-sputter yields on CIEL surface (CASTEM, based on TRIM data) vs incident C charge. (inset) C flux distribution for indicated case.

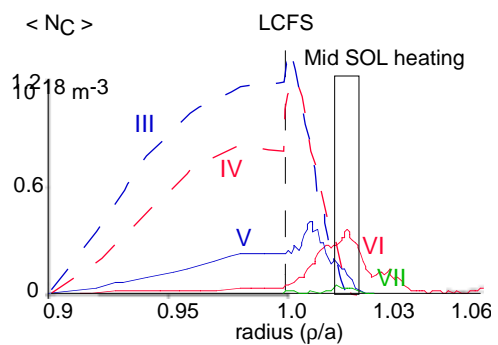


Figure 5. Radial profile of C ionization stages for case of localized SOL heating